Hepatology International (2023) 17:833–849
https://doi.org/10.1007/s12072-023-10513-0

ORIGINAL ARTICLE

Liver-derived extracellular vesicles from patients with hepatitis B virus-related acute-on-chronic liver failure impair hepatic regeneration by inhibiting on FGFR2 signaling via miR-218-5p

Senquan Zhang[1] · Jie Yu[2] · Keqiang Rao[1] · Jie Cao[1] · Lijie Ma[1] · Yeping Yu[1] · Zhe Li[1] · Zhaokai Zeng[1] · Yongbing Qian[1] · Mo Chen[1] · Hualian Hang[1]

Received: 4 January 2023 / Accepted: 4 March 2023 / Published online: 13 April 2023

Abstract

Background Impaired liver regeneration in hepatitis B virus-related acute-on-chronic liver failure (HBV-ACLF) patients is closely related to prognosis; however, the mechanisms are not yet defined. Liver-derived extracellular vesicles (EVs) may be involved in the dysregulation of liver regeneration. Clarifying the underlying mechanisms will improve the treatments for HBV-ACLF.

Methods EVs were isolated by ultracentrifugation from liver tissues of HBV-ACLF patients (ACLF_EVs) after liver transplantation, and their function was investigated in acute liver injury (ALI) mice and AML12 cells. Differentially expressed miRNAs (DE-miRNAs) were screened by deep miRNA sequencing. The lipid nanoparticle (LNP) system was applied as a carrier for the targeted delivery of miRNA inhibitors to improve its effect on liver regeneration.

Results ACLF_EVs inhibited hepatocyte proliferation and liver regeneration, with a critical role of miR-218-5p. Mechanistically, ACLF_EVs fused directly with target hepatocytes and transferred miR-218-5p into hepatocytes, acting by suppressing *FGFR2* mRNA and inhibiting the activation of ERK1/2 signaling pathway. Reducing the level of miR-218-5p expression in the liver of ACLF mice partially restored liver regeneration ability.

Conclusion The current data reveal the mechanism underlying impaired liver regeneration in HBV-ACLF that promotes the discovery of new therapeutic approaches.

Senquan Zhang, Jie Yu, Keqiang Rao and Jie Cao have contributed equally to the research.

✉ Yongbing Qian
qianyb79@hotmail.com

✉ Mo Chen
chenmo@renji.com

✉ Hualian Hang
hanghualian@shsmu.edu.cn

[1] Department of Liver Surgery, Renji Hospital, School of Medicine, Shanghai Jiao Tong University, Shanghai 200127, China

[2] Department of Endocrinology, Renji Hospital, School of Medicine, Shanghai Jiao Tong University, Shanghai 200127, China

Graphical abstract

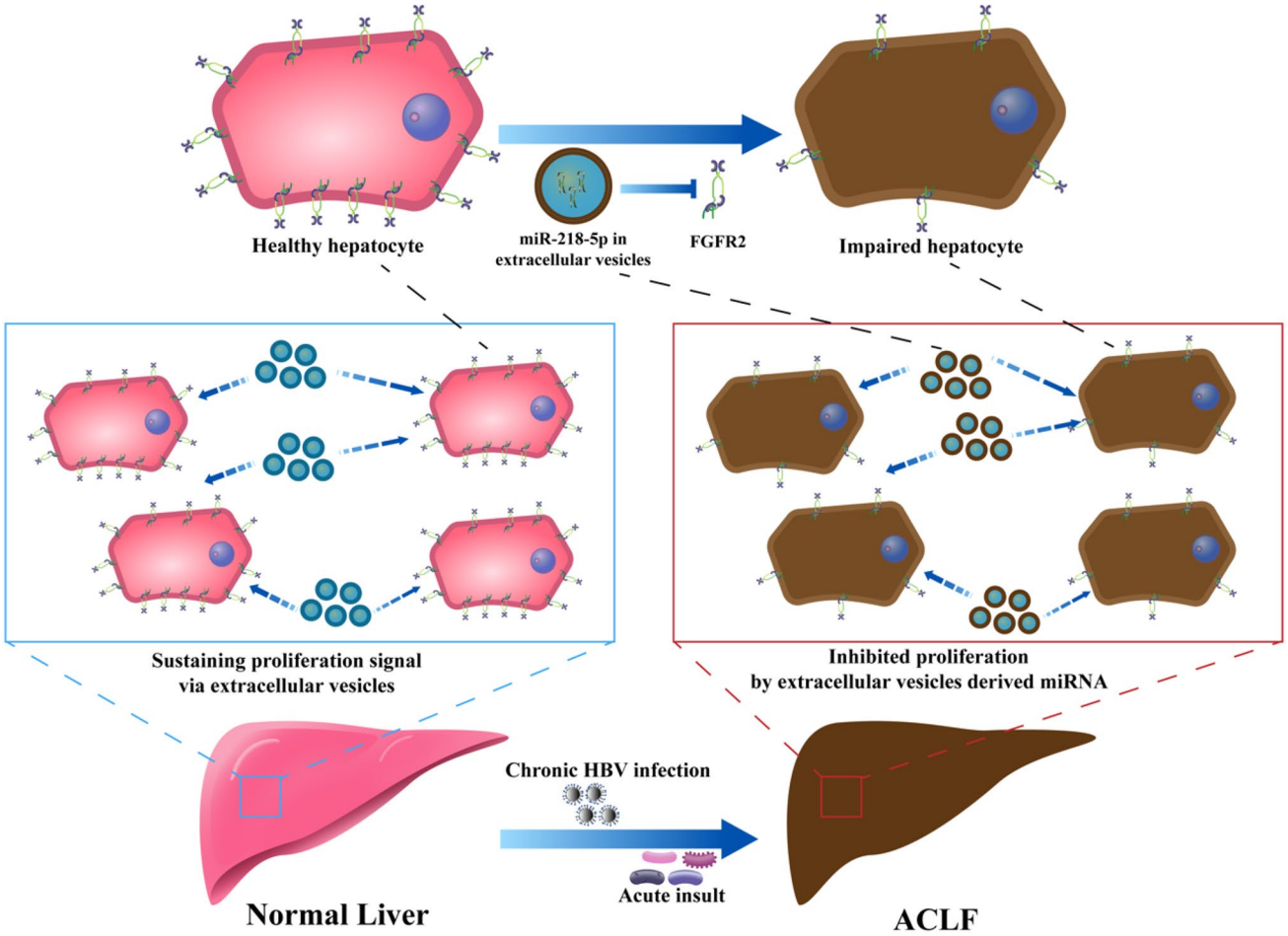

Keywords Acute-on-chronic liver failure · Liver regeneration · Extracellular vesicles · miR-218-5p · Hepatitis B virus · FGFR2 · Lipid nanoparticle · ERK1/2 · miRNA sequencing · Liver cirrhosis

Abbreviations

CCl_4	Carbon tetrachloride
ALT	Alanine aminotransferase
AST	Aspartate aminotransferase
LDH	Lactate dehydrogenase
TBIL	Total bilirubin
BUN	Blood urea nitrogen
ACLF	Acute-on-chronic liver failure
HC	Healthy control
CI	Chronic inflammation
EVs	Extracellular vesicles
ACLF_EVs	Liver-derived extracellular vesicles from ACLF
HC_EVs	Liver-derived extracellular vesicles from healthy control
H&E staining	Hematoxylin–eosin staining
PCNA	Proliferating cell nuclear antigen
CCK-8	Cell Counting Kit-8
DAPI	4′,6-Diamidino-2-phenylindole
EdU	5-Ethynyl-2′-deoxyuridine
LC	Liver cirrhosis
LC_EVs	Liver-derived extracellular vesicles from LC
DE-miRNAs	Differentially expressed miRNAs
KEGG	Kyoto Encyclopedia of Genes and Genomes
GO	Gene ontology
FGFR2	Fibroblast Growth Factor Receptor 2
ALB	Albumin
miR_veh	miR-vehicle
miR_inh	miR-inhibitor
miR_ago	miR-agomir
miR_ant	miR-antagomir

LNP	Lipid nanoparticle
NPCs	Nonparenchymal cells

Introduction

Acute-on-chronic liver failure (ACLF) is a unique disease characterized by acute deterioration of liver function, extrahepatic organ failure, and high short-term mortality [1]. It usually occurs as a result of acute liver injury on the basis of long-term chronic liver disease. In China, the most common chronic underlying liver diseases are chronic hepatitis B (CHB) and hepatitis B virus-related liver cirrhosis (HBV-LC), while alcoholic-related liver disease is predominant in Europe and the USA [2]. The major acute injuries include acute reactivation of hepatitis B virus (HBV), accumulation of hepatotoxic drugs, and acute bacterial infection [3]. Since the pathogenesis of ACLF is yet to be elucidated, liver transplantation is still the only clinical cure for HBV-ACLF [4]. The occurrence and development of HBV-ACLF involves several mechanisms. The current study on HBV-ACLF mainly focuses on intrahepatic injury, immune dysregulation, and systemic inflammatory response syndrome (SIRS). As a key factor affecting the prognosis of HBV-ACLF, impaired liver regeneration remains poorly studied [3].

The healthy liver has a high capacity for regeneration in response to acute injury [5]. Several studies reported that healthy liver is capable of repairing the injury part on its own to restore the normal size and function under different kinds of acute injuries, including drug-induced injury, hepatic resection, and ischemia–reperfusion injury. Self-replication of quiescent differentiated hepatocytes is the primary form of regeneration in healthy liver [6]. This process is regulated by multiple mechanisms, and signals are transmitted among cells through various signaling mediators to regulate liver regeneration. Normal regulatory signals for liver regeneration contribute to recovery from the disease. However, studies on liver regeneration in ACLF demonstrated that due to long-term chronic liver injury, self-replication of healthy hepatocytes in the liver is inhibited, followed by the compensatory proliferation of liver progenitor cells [3]. In this state, liver reserve function is severely lost, and when facing acute damage, the residual liver function is unable to compensate, leading to the onset of severe organ failure. Studies on ACLF mice have shown that their livers have impaired regenerative capacity due to STAT1/STAT3 imbalance, and treatment with IL-22fc could stimulate liver regeneration and alleviate symptoms [7]. Evidently, multiple abnormal liver regeneration signals are present in vivo during the course of ACLF that inhibit the self-replication of healthy hepatocytes, resulting in insufficient liver regeneration capacity. Therefore, further study of abnormal mechanism of liver regeneration in ACLF is necessary for disease management.

Extracellular vesicles (EVs), critical signaling mediators in vivo, are composed of phospholipid bilayers with a diameter of 30–150 nm [8]. Almost all cells have the ability to secrete EVs. The regulatory function of EVs has been confirmed by many studies. However, current studies mainly focus on EVs secreted by different types of cells cultured in vitro. For example, Zhou et al. found that ICC cell-derived EVs induce immunosuppressive macrophages to promote tumor progression [9]. In addition, EVs are closely associated with liver regeneration and those secreted by cultured primary hepatocytes have the ability to promote cell proliferation [10]. Also, EVs from mesenchymal stem cells [11], HepG2 cells [12], and other cell lines contributed to liver regeneration. However, due to differences in the cell growth microenvironment, EVs secreted by cultured cells in vitro do not fully reflect the disease condition. Therefore, the nascent concept of EVs extracted from the tissue has recently attracted significant attention from researchers. These EVs are secreted in response to changes in the body's microenvironment and transported to neighboring cells within the organ or to other distal organs via blood circulation. A recent study reported that EVs extracted from adipose tissue could be transported to the brain and promote cognitive impairment in mice with insulin resistance [13]. This finding suggested that EVs are crucial for signaling transmission between different tissues in vivo. EVs in vivo transmit negative regulatory signals leading to exacerbation of disease. In addition, it was found that liver-derived EVs from healthy mice and CCl_4-induced liver-injured mice promote liver regeneration, suggesting a role of EVs in regulating liver regeneration [14]. In conclusion, in vivo EVs are intercellular signaling materials with critical functions in the maintenance of a healthy microenvironment and in the development of disease. Therefore, we speculated a link between liver-derived EVs and impaired liver regeneration in HBV-ACLF patients.

The content of EVs mainly includes mRNAs, miRNAs, and small molecule proteins, which are involved in intercellular signaling through various pathways, such as cellular autocrine and paracrine secretion [15]. miRNAs are crucial components with regulatory functions within EVs. Several studies have reported that miRNAs are closely related to liver regeneration [16]. Ng et al. demonstrated that miR-21 promotes liver regeneration by improving the expression of cyclinD1 [17]. Chang et al. showed that the loss of hepatic miR-194 promotes liver regeneration in acetaminophen-induced acute liver injury mice [18]. However, miRNA-related studies within the field of HBV-ACLF research were currently focused on identifying HBV-ACLF-specific biomarkers within plasma [19, 20]. Currently, only a few studies have focused on how miRNAs regulate liver regeneration in HBV-ACLF.

In this study, we found that liver-derived EVs and their cargo miRNAs from HBV-ACLF patients could inhibit liver regeneration. Next, we showed that therapeutic treatments targeting liver-derived EVs or their cargo miRNAs could significantly promote liver regeneration in ACLF mice.

Materials and methods

Human study cohort

Liver tissue of HBV-ACLF patients was obtained from postoperative discarded liver tissue after transplantation. The diagnosis of HBV-ACLF was established based on the guidelines of the Chinese Group on the Study of Severe Hepatitis B-ACLF. Healthy liver tissue was obtained from discarded donor liver tissue after living liver transplantation. All these tissues were provided by the Department of Liver Surgery, Renji Hospital, School of Medicine, Shanghai Jiao Tong University, Shanghai, China. This study was approved by the Ethics Committee of Renji Hospital, Shanghai Jiao Tong University School of Medicine (KY2022-024-B).

Animals and murine models

6–8-week-old male C57Bl/6 mice were purchased from Shanghai JieSiJie Animal Laboratory. All institutional and national guidelines for the care and use of laboratory animals were followed. Acute liver injury model was constructed by intraperitoneal injection of 50% CCl_4 (2 μL/g) into mice. The ACLF model was constructed according to the following steps. First, a mouse model of chronic liver fibrosis was established by intraperitoneal injection of 10% CCl_4 (2 μL/g) into mice twice a week for 8 weeks. Next, 20% of CCl_4 (2 μL/g) was injected intraperitoneally to induce acute injury. After 24 h, *Klebsiella pneumoniae* (*K.p.*) strain 43816 (ATCC, Manassas, VA, USA) was injected intraperitoneally to induce the ACLF model.

Isolation of EVs from the liver tissues

Liver-derived EVs were isolated as described previously [21]. Briefly, liver tissues were collected after liver transplantation immediately, sliced small pieces, and infiltrated with serum-free Dulbecco's modified Eagle medium. A multi-tissue dissociation kit (Miltenyi, EA, GER) was added according to the instruction and gently stirred at 37 °C for 30 min. This kit dissociated the liver tissue into a single-cell suspension without damaging the intrahepatic cells, thus avoiding the release of substances from the ruptured cells that might affect the purity of the EVs. Then, we used a filter with a pore size of 70 μm for the filtration step to remove the largest elements. The cells were removed by centrifugation of the remaining liquid at 800 g, 4 °C for 10 min, followed by centrifugation at 3000*g* for 20 min to remove cell debris and two times at 12,000*g* for 1 h each to remove the subcellular structures. The resulting supernatant was clarified by ultracentrifugation at 120,000*g* for 2 h. The precipitating EVs were resuspended in phosphate-buffered saline (PBS) for subsequent experiments.

Transmission electron microscopy (TEM)

Liver-derived EVs solubilized in PBS were fixed on copper grids (Electron Microscopy Sciences, Fort Washington, PA, USA) and rested for 30 min before negative staining with 2% uranyl acetate (Ted Pella, Redding, CA, USA). Data were acquired using JEM 1011 microscope (JEOL, Tokyo, Japan).

Nanoparticle tracking analysis (NTA)

Particle concentration and diameter of liver-derived EVs were determined using a Nanosight NS300 (Malvern & Nanosight NS300, UK).

Western blotting

The proteins of liver tissues and cells were extracted using RIPA Lysis Buffer (Beyotime, Shanghai, China), and the concentration was detected using BCA Protein Assay Kit (Beyotime, Shanghai, China). An equivalent of 10 μg of protein was loaded onto 10% SDS-PAGE and transferred to the nitrocellulose membrane (Beyotime, Shanghai, China). The membranes were blocked using skimmed milk and incubated with primary and secondary antibodies sequentially. Finally, we detected the proteins using Omni-ECL™ Femto Light Chemiluminescence Kit (Epizyme Biotech, Shanghai, China). Anti-CD9, anti-CD81, anti-TSG101, anti-ERK1/2, p-anti-ERK1-2, anti-CyclinD1, anti-Tubulin, and horseradish peroxidase (HRP) goat anti-rabbit IgG antibodies were purchased from Abclonal (Wuhan, China).

Quantitative polymerase chain reaction (qPCR)

Total RNA was extracted from cells and tissues using FastPure Cell/Tissue Total RNA Isolation Kit V2 (Vazyme, Nanjing, China). The quality and quantity of total RNA were detected by NanoDrop (Thermo, Wilmington, DE, USA). cDNA was synthesized using HiScript II QRT SuperMix for qPCR (Vazyme, Nanjing, China). qRT-PCR was performed using ChamQ SYBR Color qPCR Master Mix (Vazyme, Nanjing, China). The thermal cycling parameters were as follows: initial denaturation at 95 °C (10 min), followed by 40 cycles at 95 °C (15 s) and 60 °C (60 s), and the C_t values of the melting curves. C_t values were obtained. Subsequent data analysis was performed to determine the

differences between groups at the transcriptome level. The primer sequences involved in this experiment are listed in Supplementary Table S1.

Cell counting kit (CCK)-8 assay

Cells were seeded in 96-well plates at a density of 3000 cells/well. After treatment with EVs or miRNA, the medium was replaced with a fresh medium containing 10% CCK-8 reagent (Beyotime, Shanghai, China). After incubation, the absorbance was measured at OD450 nm on a microplate reader.

EdU cell proliferation assay

Cells were seeded in 48-well plates at a density of 5000 cells/well. After treatment with EVs or miRNA, Beyo-Click™ EdU Cell Proliferation Kit reagent with Alexa Fluor 488 (Beyotime, Shanghai, China) was added to the medium. The intensity of green fluorescence was observed under a fluorescent microscope to analyze the state of cell proliferation.

Tracing of EVs

An equivalent volume of PKH26 Green Fluorescent Cell Linker Mini Kit (Fluorescence Biotechnology, Beijing, China) reagent was added to the EVs dissolved in PBS and incubated at room temperature for 5 min. An equivalent volume of 1% bovine serum albumin (BSA, Beyotime, Shanghai, China) was added to terminate the staining, followed by centrifugation at 120,000*g* 4 °C for 1 h. The precipitate of PKH67-labeled cells (Fluorescence Biotechnology, Beijing, China) was treated with the stained EVs for 24 h. The absorption of EVs was observed under a confocal laser scanning microscope (Leica, GER).

Measurement of serum enzyme activity

The enzymatic activities of alanine aminotransferase (ALT), aspartate aminotransferase (AST), the level of lactate dehydrogenase (LDH), total bilirubin (TBIL) and blood urea nitrogen (BUN) were measured by ELISA kits (Nanjing Jiancheng Institute of Biological Engineering, Nanjing, China) according to the manufacturer's instructions.

Histological analysis and immunohistochemistry

Liver tissue was fixed in 10% formalin, embedded in paraffin, and cut into 4-μm-thick sections. The sections were stained with hematoxylin and eosin (HE) and scored for histopathological changes. Immunohistochemical analysis was performed as described previously [22]. Briefly, the liver sections were incubated with anti-PCNA or anti-Ki67 primary antibodies before incubation with the corresponding secondary antibodies. The stained sections were visualized using DAB Horseradish Peroxidase Color Development Kit (Beyotime, Shanghai, China) at room temperature, and the images were observed under an inverted microscope. The quantitative results were evaluated using ImageJ (Media Cybernetics, Silver Springs, MD, USA). All antibodies used in this experiment were purchased from Abclonal (Wuhan, China).

Dual-luciferase reporter assay

Wild-type (WT) or mutant (MUT) 3'-UTR of FGFR2 as cloned and constructed into the pGL3-Luc luciferase vector (Promega, USA). 293T cells were transfected with a luciferase vector along with miR-218-5p mimic or miR-vehicle. At 48 h post-transfection, the relative luciferase activity was analyzed using a dual-luciferase reporter assay kit (Promega, USA).

Isolation of primary mouse hepatocytes and non-parenchymal cells (NPCs)

Prepare in advance 40 ml of EGTA solution (solution A) and 45 ml of GBSS supplemented with 37.5 mg of collagenase 1 (solution B). Add 3 ml solution B to 24 ml GBSS and label as solution C. Store liquid A, liquid B and liquid C at a constant temperature of 37 °C. Mice were anesthetized and the abdominal cavity was opened to locate the portal vein. The infusion tube was inserted into the portal vein and secured. Aspirate 30 ml of solution A, cut open the inferior vena cava, and instill fluid A along the portal vein within 3 min. The liver tissue was removed and put into solution C, cut up and shaken at 100 rpm for 5 min. 70 μm filter was used and centrifuged at 4 °C 500 rpm for 3 min to filter tissue. The supernatant was discarded, GBSS was added and centrifuged at 4 °C 500 rpm for 5 min. The precipitate was collected and the isolated hepatocytes were obtained. The supernatant was centrifuged at 4 °C 4000 rpm for 5 min. Collect the precipitate, which is the NPCs.

Statistical analysis

Statistical analysis was performed using GraphPad Prism software (version 8). All values are expressed as mean ± standard deviation (SD) ($n \geq 3$ experiments). Statistical significance was determined using Student's *t* test and one-way analysis of variance (ANOVA). n.s., no significance, $*p < 0.05$, $**p < 0.01$, $***p < 0.001$.

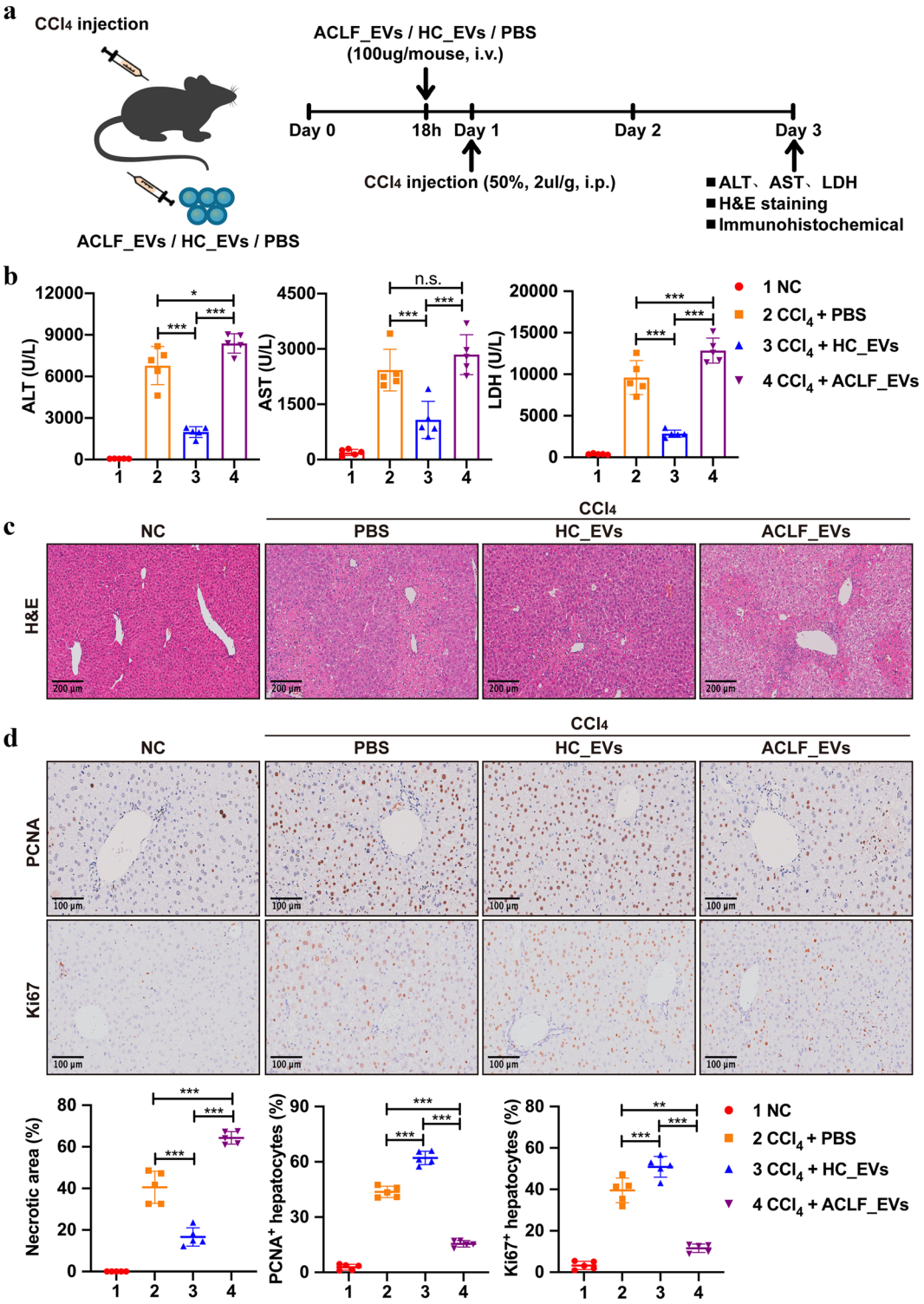

Results

Liver-derived EVs from HBV-ACLF patients inhibited liver regeneration

To determine whether liver-derived EVs were associated with impaired liver regeneration of HBV-ACLF, we collected discarded liver tissues from HBV-ACLF patients after liver transplantation. Healthy livers were collected as controls. Liver-derived EVs of HBV-ACLF and healthy controls (ACLF_EVs and HC_EVs) were extracted from the liver tissue as described previously. Then, we analyzed

◂**Fig. 1** Liver-derived EVs from HBV-ACLF patient inhibited liver regeneration in ALI mice. **a** Schematic diagram of the procedure. C57BL/6 mice were treated with EVs or PBS solution via tail vein injection for 6 h, followed by intraperitoneal injection of 50% CCl_4 or olive oil to induce ALI: groups: 1, PBS and olive oil; 2, PBS and CCl_4; 3, HC_EVs and CCl_4; 4, ACLF_EVs and CCl_4. **b** Liver function tests of ALT, AST, and LDH showed slowed liver self-repair after ACLF_EVs treatment ($n=5$). **c** H&E staining showed increased area of liver necrosis after ACLF_EVs treatment ($n=5$). Scale bars, 200 μm. **d** Immunohistochemistry staining of PCNA and Ki67 showed impaired liver regeneration after ACLF_EVs treatment ($n=5$). Scale bars, 100 μm. Quantitative presentation of necrotic area, $PCNA^+$ or $ki67^+$ hepatocytes were shown. One-way ANOVA was used for statistical evaluation (n.s., no significance; $^*p<0.05$; $^{**}p<0.01$; $^{***}p<0.001$). Data were presented as the mean ± SD. *CCl_4* carbon tetrachloride, *ALT* alanine aminotransferase, *AST* aspartate aminotransferase, *LDH* lactate dehydrogenase, *ACLF* acute-on-chronic liver failure, *HC* healthy control, *EVs* extracellular vesicles, *ACLF_EVs* liver-derived extracellular vesicles from ACLF, *HC_EVs* liver-derived extracellular vesicles from healthy control, *H&E staining* hematoxylin–eosin staining, *PCNA* proliferating cell nuclear antigen

the physicochemical features of the ACLF_EVs and HC_EVs. Under Transmission Electron Microscope (TEM), both ACLF_EVs and HC_EVs showed clear cup sharp (Fig. S1a), and nanoparticle tracking analysis (NTA) showed that their diameter was about 130 nm (Fig. S1b). Western blot showed that both ACLF_EVs and HC_EVs were positive for classical EVs markers, such as CD9, CD81, and TSG101 (Fig. S1c). This indicated that there were no differences between ACLF_EVs and HC_EVs in terms of markers, morphology, and diameter.

Lee et al. [14] used a classical 50% CCl_4-induced acute liver injury (ALI) mouse model for liver regeneration studies to demonstrate that liver-derived EVs could promote liver regeneration. Therefore, to explore whether ACLF_EVs had functions that affected liver regeneration, we injected ACLF_EVs (ACLF_EVs group) and HC_EVs (HC_EVs group) into ALI mice through the tail vein to observe the pathological changes of the liver (Fig. 1a). About 100 μg EVs were injected 6 h before intraperitoneal injection of CCl_4, while PBS (PBS group) was used as the blank control. The mice were sacrificed after 48 h. The markers of liver injury were detected in the plasma. Compared to the PBS group, ALT, AST, and LDH were upregulated in the ACLF_EVs group ($p<0.05$) but were significantly downregulated in the HC_EVs group (Fig. 1b, $p<0.001$). In addition, HE staining of liver tissue showed similar results (Fig. 1c). The intraperitoneal injection of CCl_4 could induce severe liver necrosis, while in the ACLF_EVs group, the area of liver necrosis was further enlarged. On the contrary, HC_EVs exerted a protective effect on liver injury, reducing the area of liver necrosis. This finding proved that ACLF_EVs could aggravate the degree of liver injury in ALI mice. During ALI, hepatocytes rapidly enter the cell cycle and proliferate to repair liver injury. Therefore, PCNA and ki67 staining were used to detect the proliferation of hepatocytes. As shown in Fig. 1d, the number of PCNA-positive hepatocytes was significantly decreased in the ACLF_EVs group but increased in the PBS and HC_EVs group. Ki67 staining showed similar results. In conclusion, the current results showed that ACLF_EVs were negatively correlated with liver injury repair by inhibiting liver regeneration.

Liver-derived EVs from HBV-ACLF patients suppressed the proliferation of hepatocytes in vitro

As the main parenchymal cells of liver tissue, hepatocytes play a critical role in the process of liver regeneration. Therefore, we attempted to determine the effect of ACLF_EVs on hepatocytes in vitro using AML12 cells, a normal mouse hepatocyte line. Some studies have shown that EVs primarily rely on fusion with membranes of target cells to deliver substances to effectuate regulatory functions. Therefore, we investigated whether ACLF_EVs can bind to AML12 cells. Hence, PKH26 dye (a fluorescent red linker compound) was used to label ACLF_EVs and HC_EVs, and PKH67 dye (a fluorescent green linker compound) was used to label the membranes of AML12 cells in vitro. Both ACLF_EVs and HC_EVs were co-cultured with AML12 cells at a concentration of 25 μg/mL for 24 h. Laser confocal microscopy showed that the cell membrane of AML12 cells excited both red and green fluorescence signals, indicating that EVs were successfully absorbed into the cells (Fig. 2a). Then, ACLF_EVs and HC_EVs were co-cultured with AML12 cells at different concentration gradients to explore their effects on the proliferation of AML12 cells. CCK-8 assay showed that the proliferation of AML12 cells was significantly downregulated in an ACLF_EVs concentration-dependent manner compared to PBS treatment (Fig. 2b). Conversely, the proliferation ability of AML12 cell was significantly improved within increasing concentrations of HC_EVs (Fig. 2b). In addition, similar results were observed with EdU staining assay of AML12 cells (Fig. 2c). The ACLF_EVs treatment resulted in a significant decrease in EdU incorporation and significant downregulation of the green fluorescence ratio in AML12 cells, while the opposite result was obtained after HC_EVs treatment. In summary, in vitro studies revealed that liver-derived EVs regulated hepatocyte proliferation. ACLF_EVs could deliver negative proliferative signals to inhibit hepatocyte proliferation, suggesting their role in the regeneration inhibition of HBV-ACLF.

miRNA in liver-derived EVs from HBV-ACLF patients dominated the inhibition of liver regeneration

miRNAs are highly conserved among different species and are abundant in EVs, playing a pivotal role in the regulation of recipient cells. Based on their important regulatory

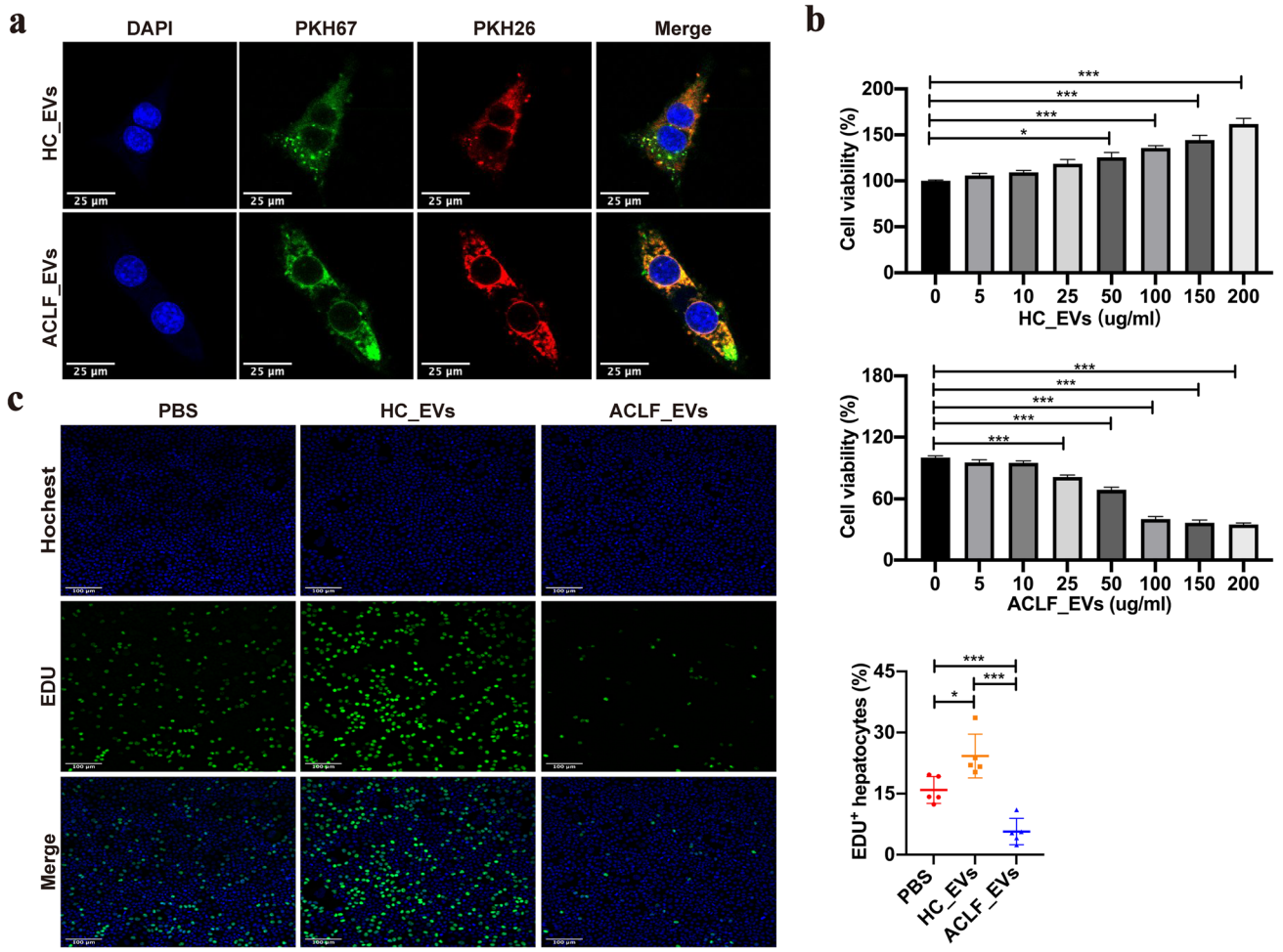

Fig. 2 Liver-derived EVs from HBV-ACLF patient inhibited hepatocyte proliferation. **a** HC_EVs and ACLF_EVs were stained with PKH26 (red) and incubated with AML12 cells pre-stained with PKH67 (green) for 24 h, and EVs uptake was observed under Confocal laser scanning microscope. Scale bars, 25 μm. **b** CCK-8 assay showed inhibition of hepatocyte proliferation after treatment with ACLF_EVs. **c** EdU cell proliferation assay showed impaired proliferation of hepatocytes after treatment with ACLF_EVs. Scale bars, 100 μm. Quantitative presentation of EdU^+ AML12 cells were shown ($n=5$). One-way ANOVA was used for statistical evaluation ($^*p<0.05$; $^{***}p<0.001$). Data were presented as the mean ± SD. *ACLF_EVs* liver-derived extracellular vesicles from ACLF, *HC_EVs* liver-derived extracellular vesicles from healthy control, *CCK-8* Cell Counting Kit-8, *DAPI* 4′,6-diamidino-2-phenylindole, *EdU* 5-ethynyl-2′-deoxyuridine

status, the miRNAs in ACLF_EVs and HC_EVs were profiled using deep RNA sequencing to identify the candidates responsible for liver regeneration. A total of 106 differentially expressed miRNAs (DE-miRNAs) were identified between ACLF_EVs and HC_EVs. Among them, 58 miRNAs were upregulated and 48 were downregulated in ACLF_EVs compared to HC_EVs (Fig. 3a). The target genes of these DE-miRNAs were predicted by miRanda and RNAhybrid. Gene Ontology (GO) and Kyoto Encyclopedia of Genes and Genomes (KEGG) enrichment analysis on these target genes were applied to investigate the function of these miRNAs. GO enrichment analysis suggested that the target genes of DE-miRNAs were closely related to regeneration-related signaling modules, such as cell–cell signaling, cell morphogenesis, and regulation of multicellular organismal development (Fig. S2a). KEGG enrichment analysis revealed that the target genes of DE-miRNAs were enriched in proliferation-related signaling pathways, such as MAPK and Rap1 signaling pathway (Fig. 3a). Therefore, we suggested that DE-miRNAs were critical in ACLF_EVs that regulated liver regeneration.

ACLF often occurred acutely in the setting of liver cirrhosis (LC). In this stage, persistent chronic injury impaired the ability of healthy hepatocytes to self-replicate, resulting in a severe decrease in the liver reserve function, which prevents compensatory liver regeneration in the face of acute injury. This implied a similar state of inhibition of regeneration in the diseased liver during the LC phase. Therefore,

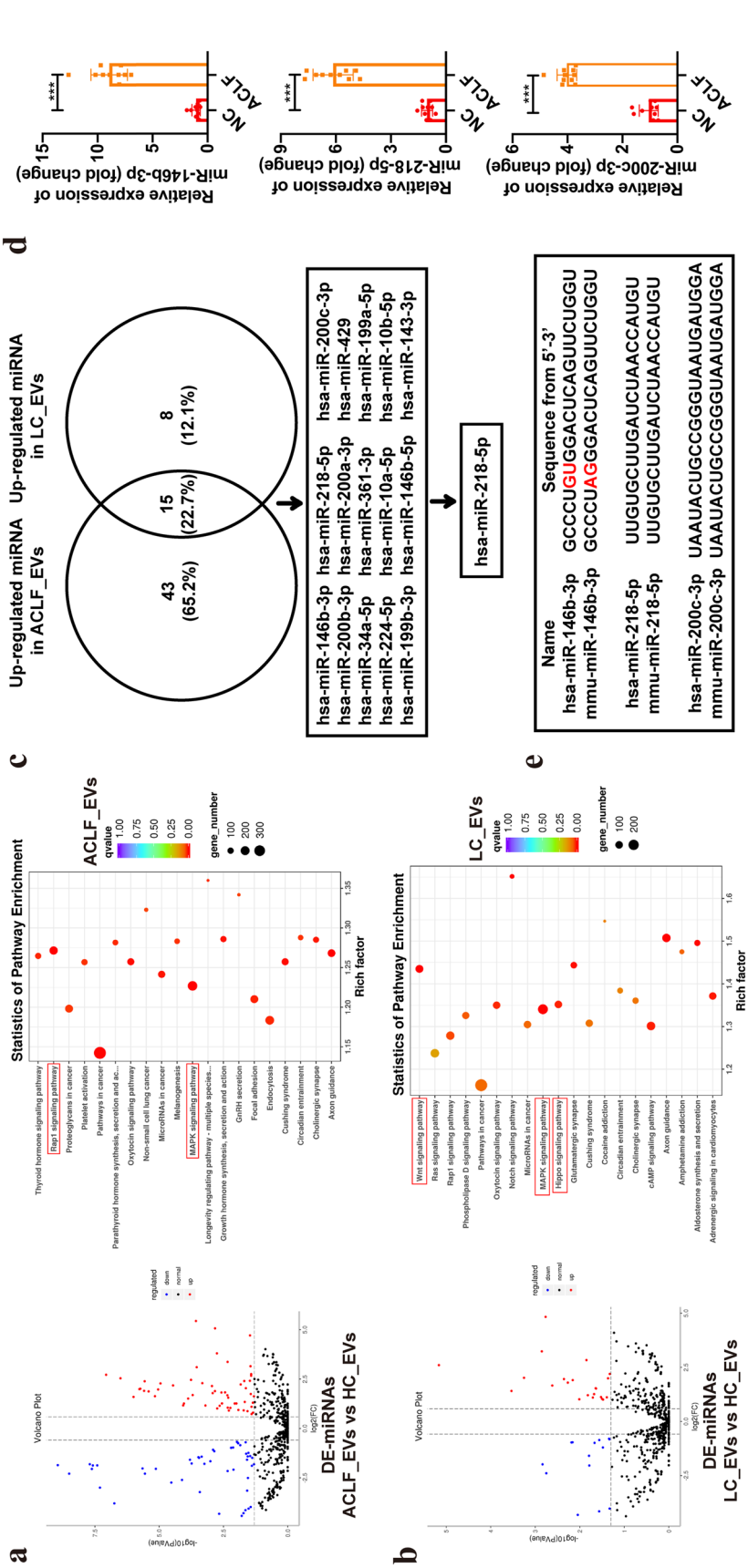

Fig. 3 miR-218-5p was the most important functional miRNA within ACLF_EVs. **a** Volcano plot showed the number of DE-miRNAs within ACLF_EVs. KEGG enrichment analysis of DE-miRNAs within ACLF_EVs. **b** Volcano plot showed the number of DE-miRNAs within LC_EVs. KEGG enrichment analysis of DE-miRNAs within LC_EVs. **c** Key miRNA screening procedure: miRNAs upregulated both in ACLF_EVs and LC_EVs. **d** qPCR for DE-miRNAs ($n = 10$). **e** Sequence comparison of human and mouse-derived miRNAs. One-way ANOVA was used for statistical evaluation (***$p < 0.001$). Data were presented as the mean ± SD. *LC* liver cirrhosis, *ACLF_EVs* liver-derived extracellular vesicles from ACLF, *LC_EVs* liver-derived extracellular vesicles from LC, *HC_EVs* liver-derived extracellular vesicles from healthy control, *DE-miRNAs* differentially expressed miRNAs, *KEGG* Kyoto Encyclopedia of Genes and Genomes

we extracted EVs from the liver tissue of LC patients (LC_EVs) and co-cultured with AML12 cells in vitro. EdU staining assay revealed that similar to ACLF_EVs, LC_EVs could also inhibit hepatocyte proliferation (Fig. S3a). The expression of miRNAs in LC_EVs was profiled using deep RNA sequencing, wherein 37 DE-miRNAs were identified between LC_EVs and HC_EVs. Among them, 23 miRNAs were upregulated and 14 were downregulated in LC_EVs compared to HC_EVs (Fig. 3b). GO enrichment analysis revealed that the target genes of DE-miRNAs were closely related to the regulation of cell differentiation, multicellular organismal development, cell development, and other modules (Fig. S2b). KEGG enrichment analysis suggested that the target genes of DE-miRNAs were mainly enriched in MAPK, WNT and HIPPO signaling pathway, which were closely associated with regeneration (Fig. 3b). Since miRNAs degraded mRNAs and thus, inhibited protein translation and synthesis mainly through partial complementary binding to the 3′ non-coding regions [3′ untranslated regions (UTRs)] of target mRNAs, we focused on DE-miRNAs upregulated in ACLF_EVs and LC_EVs. Next, we searched for DE-miRNAs that were upregulated in both ACLF_EVs and LC_EVs. Finally, 15 miRNAs were screened (Fig. 3c); among these, 3 miRNAs (miR-146b-3p, miR218-5p and miR-200c-3p) were significantly upregulated ($p < 0.05$ and $Log_2FC > 2$). The expression of these three miRNAs in ACLF_EVs and HC_EVs was demonstrated by qPCR. Compared to HC_EVs, all these three miRNAs increased significantly in ACLF_EVs ($p < 0.001$) (Fig. 3d). In addition, we compared the sequences of these miRNAs between humans and mice (Fig. 3e) and found that the sequence of has-miR-146b-3p and mmu-miR-146b-3p did not match exactly, suggesting that miR-146b-3p was not conserved between different species, while miR-218-5p and miR-200c-3p were highly conserved across species. Thus, we suggested that miR-218-5p, the most significant DE-miRNA, might be the major factor in ACLF_EVs that inhibited liver regeneration.

miR-218-5p exerted an inhibitory effect in liver regeneration mediated by liver-derived EVs from HBV-ACLF patients

To investigate whether miR-218-5p could regulate hepatocyte proliferation, we transfected AML12 cells in vitro with miR-218-5p-mimic to observe its function on liver regeneration. The CCK-8 assay revealed that the proliferation of AML12 cells transfected with miR-218-5p-mimic (miR_mimic group) was significantly inhibited compared to cells transfected with miR-218-5p-vehicle (miR_veh group) (Fig. 4a). Similarly, EdU staining assay revealed a significant reduction in green fluorescence in the miR_mimic group (Fig. 4b). These results confirmed that miR-218-5p could inhibit the proliferation of hepatocytes. In order to further determine the function of miR-218-5p, we injected miR-218-5p-agomir (miR_ago, a powerful miRNA mimic) into ALI mice by tail vein injection to investigate its effect on liver regeneration. Moreover, immunohistochemical staining of mouse liver for PCNA and Ki67 revealed that miR-218-5p inhibited liver regeneration in mice (Fig. 4c). Next, we aimed to investigate whether miR-218-5p was crucial for ACLF_EVs inhibition of hepatocyte proliferation. Thus, ACLF_EVs were co-cultured with AML12 cells, while using miR-218-5p-inhibitor (miR_inh, an inhibitory nucleic acid fragment of miR-218-5p) to transfect AML12 cells, in order to observe whether competitive inhibition of miR-218-5p, which is highly expressed within ACLF_EVs, could antagonize the inhibitory effect of ACLF_EVs on hepatocyte proliferation. CCK-8 assay revealed that ACLF_EVs significantly inhibited the proliferation of AML12 cells, while miR-218-5p-inhibitor transfection reversed this phenomenon, which could not be restored after miR-veh transfection (Fig. 4d). Similar results were observed for EdU staining assay (Fig. 4e). In addition, we also injected ACLF_EVs and miR-218-5p-antagomir (miR_ant, a powerful miRNA inhibitor) together into ALI mice. Immunohistochemical staining for PCNA and Ki67 suggested that competitive inhibition of miR-218-5p, highly expressed within ACLF_EVs, effectively reversed the inhibitory effect of ACLF_EVs on liver regeneration (Fig. 4f). Therefore, we suggested that miR-218-5p is a key factor in ACLF_EVs that exerts regenerative inhibitory ability.

miR-218-5p inactivated the ERK1/2 signaling pathway by targeting FGFR2

Next, we attempted to identify how miR-218-5p regulated hepatocyte proliferation. Typically, miRNA regulates cell function by repressing the target mRNA. Therefore, it was crucial to identify the target mRNA of miR-218-5p that inhibited hepatocyte proliferation. We used TargetScan tool to predict the target genes of hsa-miR-218-5p, and a total of 1102 potential target genes were detected. In addition, we performed single-cell RNA sequencing of liver tissues from HBV-ACLF patients and healthy humans to observe the actual changes in the expression of mRNA. The subpopulation of hepatocytes was sorted from the data of single-cell RNA sequencing of liver tissues, and the differential changes in mRNAs were compared between HBV-ACLF and healthy humans. Subsequently, 469 differentially expressed mRNAs (DE-mRNAs, $p < 0.05$ and $Log_2FC > 0.5/Log_2FC < -0.5$) were screened, of which 198 DE-mRNAs were downregulated and 271 were upregulated. Since the function of miRNAs was to repress target mRNAs, we focused on the downregulated part of DE-mRNAs. In order to predict the function of miRNAs accurately, the species with conserved miRNAs must be considered while screening target mRNAs.

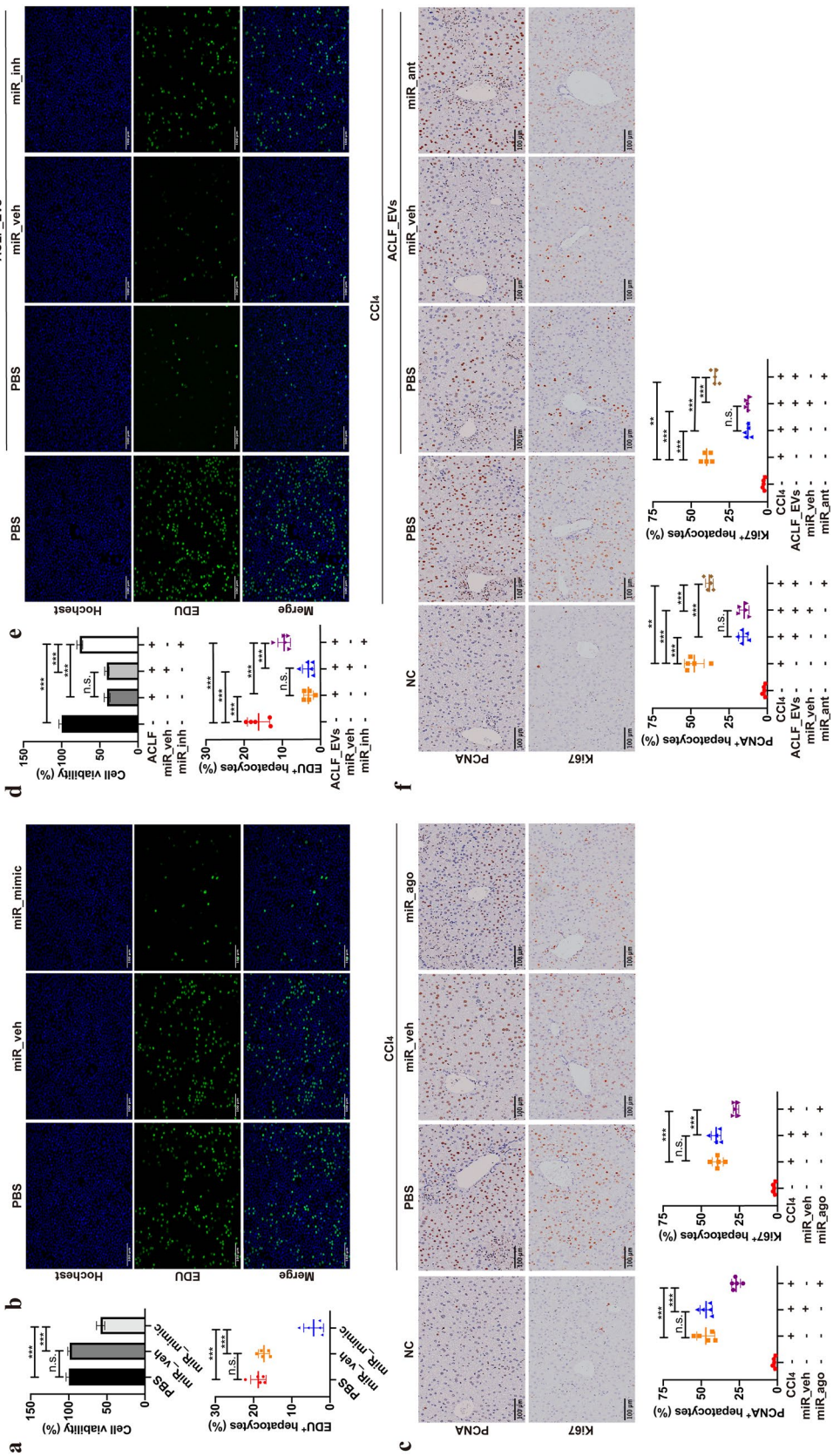

Fig. 4 miR-218-5p was a key factor in the inhibition of hepatocyte proliferation by ACLF_EVs. **a** CCK-8 assay showed inhibition of hepatocyte proliferation after treatment with miR-218-5p-mimic. **b** EdU cell proliferation assay showed impaired proliferation of hepatocytes after treatment with miR-218-5p-mimic. Scale bars, 100 μm. Quantitative presentation of EdU^+ AML12 cells were shown ($n = 5$). **c** Immunohistochemistry staining of PCNA and Ki67 showed impaired liver regeneration after miR-218-5p-agomir treatment ($n = 5$). Scale bars, 100 μm. Quantitative presentation of $PCNA^+$ or $ki67^+$ hepatocytes were shown. **d** CCK-8 assay demonstrated that miR-218-5p-inhibitor reversed decreased hepatocyte proliferation induced by ACLF_EVs. **e** EdU cell proliferation assay showed that miR-218-5p-inhibitor reversed impaired hepatocyte proliferation induced by ACLF_EVs. Scale bars, 100 μm. Quantitative presentation of EdU^+ AML12 cells were shown ($n = 5$). **f** Immunohistochemistry staining of PCNA and Ki67 showed reversed liver regeneration after miR-218-5p-antagomir treatment ($n = 5$). Scale bars, 100 μm. Quantitative presentation of $PCNA^+$ or $ki67^+$ hepatocytes were shown. One-way ANOVA was used for statistical evaluation (n.s., no significance; $^{**}p < 0.01$; $^{***}p < 0.001$). Data were presented as the mean ± SD. *ACLF_EVs* liver-derived extracellular vesicles from ACLF, *CCK-8* Cell Counting Kit-8, *DAPI* 4′,6-diamidino-2-phenylindole, *EdU* 5-Ethynyl-2′-deoxyuridine

Therefore, we assessed the target mRNAs of mmu-miR-218-5p, and a total of 963 potential target mRNAs were predicted. Next, a cross-screening of the three mRNA datasets was performed. A total of three DE-mRNAs were screened, which were significantly downregulated in the hepatocytes of ACLF patients and were potential target mRNAs for hsa/mmu-miR-218-5p (Fig. 5a). Among them, FGFR2 showed the most significant differential change and was closely associated with hepatocyte proliferation and liver regeneration (Fig. 5b) [23]. Therefore, we suggested that FGFR2 might be a potential target mRNA of miR-218-5p. Then, RNAhybrid software was utilized to predict the potential correlation between miR-218-5p and FGFR2. miR-218-5p was found to have a complementary pairing sequence at the 3′UTR of FGFR2 (Fig. 5c), and luciferase reporter assay confirmed the interaction between miR-218-5p and the 3′UTR of FGFR2 (Fig. 5d). The immunofluorescence assay was employed to observe the expression level of FGFR2 in the liver tissues of ACLF patients (Fig. 5e). Compared to NC, the expression level of FGFR2 in the hepatocytes was significantly downregulated in HBV-ACLF patients. In addition, we analyzed the level of FGFR2 in AML12 cells after transfecting with miR_mimic and found that FGFR2 level was significantly downregulated (Fig. 5f). Moreover, the downregulation of FGFR2 was reversed by transfection of miR_inh into AML12 cells co-cultured with ACLF_EVs (Fig. 5g). KEGG database suggested that ERK1/2 signaling pathway was the main downstream signaling pathway of FGFR2 and closely related to liver regeneration [24]. Also, KEGG enrichment analysis of miRNAs in ACLF_EVs suggested the importance of the MAPK signaling pathway. Therefore, we subsequently detected the changes in the ERK1/2 pathway. The results suggested that ERK1/2 activation was significantly downregulated in AML12 cells transfected with miR_mimic, and the expression of its downstream cyclinD1 was repressed (Fig. 5f). Furthermore, the activation of ERK1/2 and cyclinD1 levels was significantly decreased in AML12 cells after ACLF_EVs treatment, which was improved by transfection with miR_inh (Fig. 5g). Thus, our results suggested that miR-218-5p, highly expressed within ACLF_EVs, functioned as an inhibitor of liver regeneration by downregulating the expression of FGFR2 in the hepatocytes to suppress the activation of the ERK1/2 pathway.

Inhibition of miR-218-5p effectively enhanced liver regeneration

The current results revealed the importance of miR-218-5p; hence, we sought to investigate whether ACLF mice had similar alterations as ACLF patients. Next, we constructed an ACLF mouse model according to the method reported previously and examined the expression levels of miR-218-5p in the EVs of liver tissue from ACLF mice. The results showed that the expression of miR-218-5p was significantly increased (Fig. 6a, $p < 0.001$). Immunofluorescence assay of liver tissues also demonstrated a significant downregulation of FGFR2 level in the hepatocytes of ACLF mice (Fig. 6b).

Based on the inhibitory function of miR-218-5p on liver regeneration, we determined whether the inhibition of miR-218-5p in vivo could exert a therapeutic effect. miR-218-5p-antagomir, a specifically chemically modified miR-218-5p antagonist, inhibited the function of miR-218-5p by strongly competing with mature miR-218-5p in vivo to prevent complementary binding of miRNA with its target gene mRNA. It was administered through the tail vein, from where it is transported to the whole body through blood circulation. However, miRNAs were susceptible to degradation during transportation and could not target specific tissues and cells, markedly affecting their therapeutic effects. Yang et al. found that lipid nanoparticle (LNP) targets hepatocytes in fibrosis mice through interaction with apolipoprotein E and was subsequently internalized into hepatocytes through endocytosis [25]. Gokita et al. demonstrated the ability of LNP to deliver miRNA [26]. Therefore, to enhance its stability in vivo and its targeting ability to hepatocytes, we used LNP as a delivery system for miR-218-5p-antagomir. Subsequently, LNP-miR-218-5p-antagomir (LNP_ant group), LNP-miR-vehicle (LNP_veh group), miR-218-5p-antagomir (miR_ant group), miR-vehicle (miR_veh group), and PBS (PBS group) were administered to treat ACLF mice (Fig. 6c). Mice were sacrificed 48 h after acute CCl_4 injection. Firstly, we measured AST, ALT, TBIL and BUN in ACLF mice. The results showed that ALT, AST, and TBIL levels of Group miR_ant were reduced to some extent, and LNP delivery helped to enhance the therapeutic effect of miR_ant. No significant change in BUN was observed (Fig. S4a). To investigate liver regeneration in ACLF mice, we performed PCNA and Ki67 staining on mouse liver tissues (Fig. 6d). The results revealed that PNCA and Ki67 levels in the liver tissues of the miR_ant and LNP_ant group were significantly improved, suggesting that the inhibition of miR-218-5p enhanced the regeneration ability of the liver. Then, to verify the potential mechanism of restoration of liver regenerative capacity in ACLF mice, we conducted immunofluorescence staining on mouse liver tissues and found that in the miR_ant and LNP_ant group, FGFR2 levels in the liver tissues were significantly increased and co-localized mainly with hepatocytes (Fig. 7a). In addition, we examined the activation of ERK1/2 pathway in the liver tissues. The results showed that the p-ERK1/2 level and the downstream protein cyclinD1 were significantly upregulated in the miR_ant and LNP_ant group, suggesting that miR-218-5p inhibition in mice improves liver regeneration by increasing the activation of ERK1/2 signaling pathway (Fig. 7b).

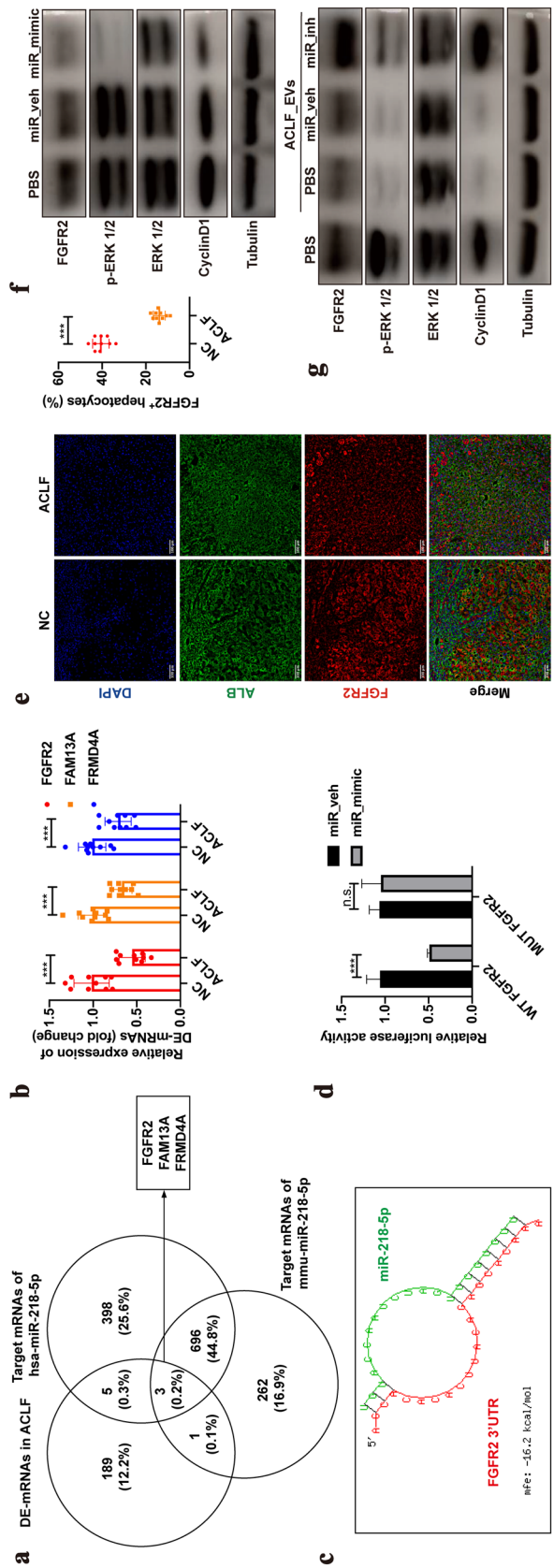

Fig. 5 miR-218-5p inhibited hepatocyte proliferation by decreasing FGFR2 expression and inactivated ERK1/2 pathway. **a** Target mRNA screening procedure: mRNAs belonging to three mRNA datasets at the same time (dataset 1, DE-mRNAs in ACLF; dataset 2, target mRNA of has-miR-218-5p; dataset 3, target mRNA of mmu-miR-218-5p). **b** Identification of mRNA expression levels by qPCR. **c** Complementary binding sequences of miR-218-5p and FGFR2. **d** Dual-luciferase reporter assay. 293T cells were transfected with miR-218-5p-mimic or miR-vehicle, together with WT or MUT 3′-UTR of FGFR2 reporter vector. The relative luciferase activity was analyzed 48 h later. **e** Immunofluorescence staining showed decreased expression of FGFR2 in hepatocytes of ACLF patients. Scale bars, 100 μm. Quantitative presentation of FGFR2$^+$ hepatocytes were shown ($n = 10$). **f** Western blotting showed that expression of p-ERK1/2 and cyclinD1 was downregulated in AML12 cells treated with miR-218-5p-mimic. **g** Western blotting showed that decreased expression of p-ERK1/2 and cyclinD1 induced by ACLF_EVs could reverse when treated with miR-218-5p-inhibitor. One-way ANOVA was used for statistical evaluation (n.s., no significance; $^{***}p < 0.001$). Data were presented as the mean ± SD. *ACLF_EVs* liver-derived extracellular vesicles from ACLF, *FGFR2* Fibroblast Growth Factor Receptor 2, *ALB* albumin, *DAPI* 4′,6-diamidino-2-phenylindole, *miR_veh* miR-vehicle, *miR_inh* miR-inhibitor

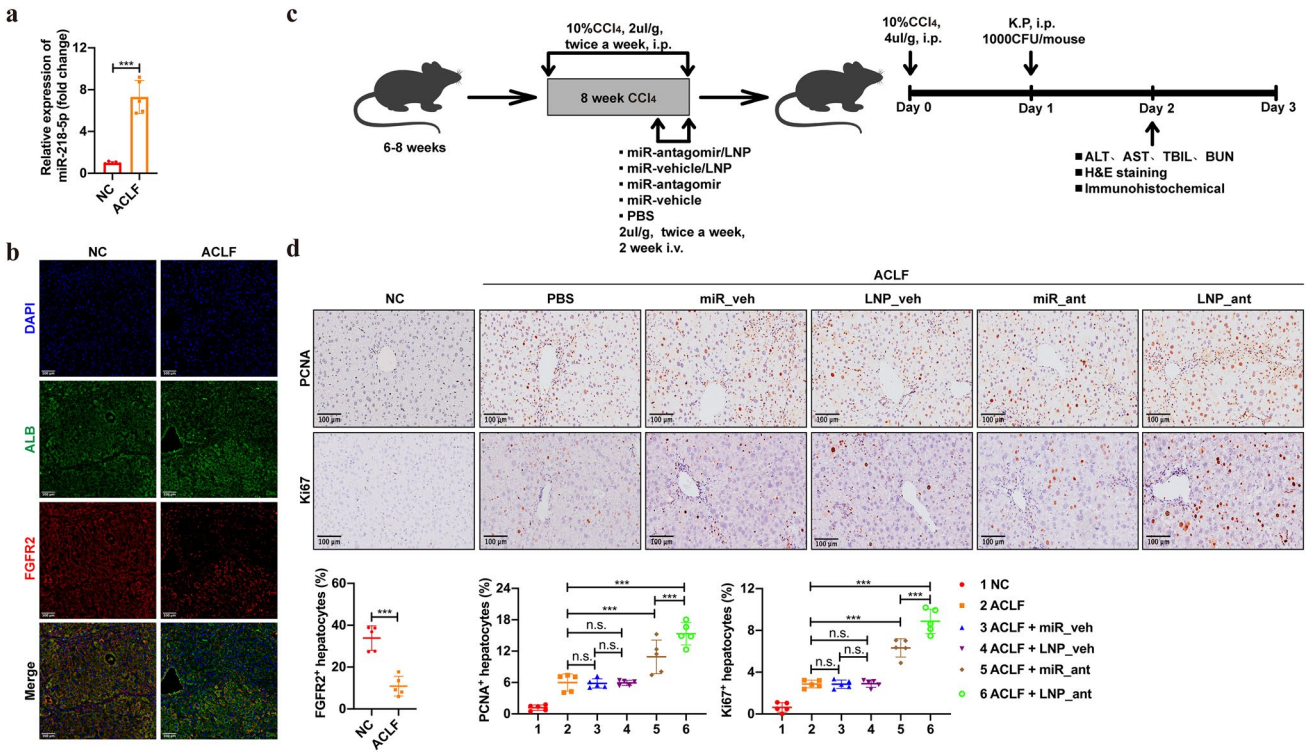

Fig. 6 Inhibition of miR-218-5p in the liver of ACLF mice could improve liver regeneration. **a** Identification of decreased expression levels of FGFR2 in ACLF mice by qPCR ($n=5$). **b** Immunofluorescence staining showed decreased expression of FGFR2 in hepatocytes of ACLF mice. Scale bars, 100 μm. Quantitative presentation of $FGFR2^+$ hepatocytes were shown ($n=5$). **c** Schematic diagram of the procedure. C57BL/6 mice treated with 10% CCl_4 for 8 weeks (twice weekly) were injected intraperitoneally with double dose of 10% CCl_4 and then 24 h later with k.p. to induce ACLF. During the 8-week CCl_4 injection phase, mice were treated with PBS or miRNA-antagomir through tail vein starting at the sixth week (twice weekly): groups: 1, NC; 2, PBS and ACLF; 3, miR_veh and ACLF; 4, LNP_veh and ACLF; 5, miR_ant and ACLF; 6, LNP_ant and ACLF. **d** Immunohistochemistry staining of PCNA and Ki67 showed that impaired liver regeneration could partially restored when treated with miR-218-5p-antagomir and the effect enhanced when delivering by LNP ($n=5$). Scale bars, 100 μm. Quantitative presentation of $PCNA^+$ and $ki67^+$ hepatocytes were shown ($n=5$). One-way ANOVA was used for statistical evaluation (n.s., no significance; $^{***}p<0.001$). Data were presented as the mean ± SD. *ACLF* acute-on-chronic liver failure, *FGFR2* Fibroblast Growth Factor Receptor 2, *ALB* albumin, *DAPI* 4′,6-diamidino-2-phenylindole, *LNP* lipid nanoparticle, *miR_veh* miR-vehicle, *miR_ant* miR-antagomir, *LNP_veh* LNP-vehicle, *LNP_ant* LNP-antagomir, *PCNA* proliferating cell nuclear antigen

Discussion

HBV-ACLF was induced by an acute hit on the liver based on long-term chronic liver disease. It was characterized by rapid progression, high mortality, and poor prognosis [1]. Several clinical studies suggested that impaired liver regeneration is a major factor contributing to the poor prognosis of HBV-ACLF. Healthy liver had a sufficient regenerative potential to repair itself through self-replication of hepatocytes after a certain degree of the strike. However, the liver suffering from chronic damage over a prolonged period has a severe loss of reserve function. As a result, when faced with an acute strike, its inability to perform rapid and effective liver regeneration leads to poor prognosis [3], indicating that restoring the reserve function of the liver and promoting liver regeneration is crucial for the treatment of HBV-ACLF. Xiang et al. constructed a mouse model that could effectively mimic the disease characteristics of clinical ACLF patients by CCl4 and *Klebsiella pneumoniae* injections [7]. The model suggested that long-term chronic liver injury and bacterial infection caused impaired liver regeneration in ACLF mice. The administration of IL-22Fc improved liver regeneration and prolonged the survival of ACLF mice. In addition, *Engelmann* et al. found that the combination of G-CSF and TLR4 inhibitors was effective in reducing inflammation and stimulating liver regeneration in ACLF mice [27]. In conclusion, finding appropriate treatments to promote liver regeneration in patients with HBV-ACLF had significant clinical translational value.

In this study, we focused on liver-derived EVs (critical cellular communication substances) and sought their potential association with impaired liver regeneration in HBV-ACLF patients. Also, liver-derived EVs were focused upon rather than EVs secreted by cell lines or primary cells. Previous studies have reported the ability of EVs secreted by primary hepatocytes or hepatocyte lines, such as HepG2

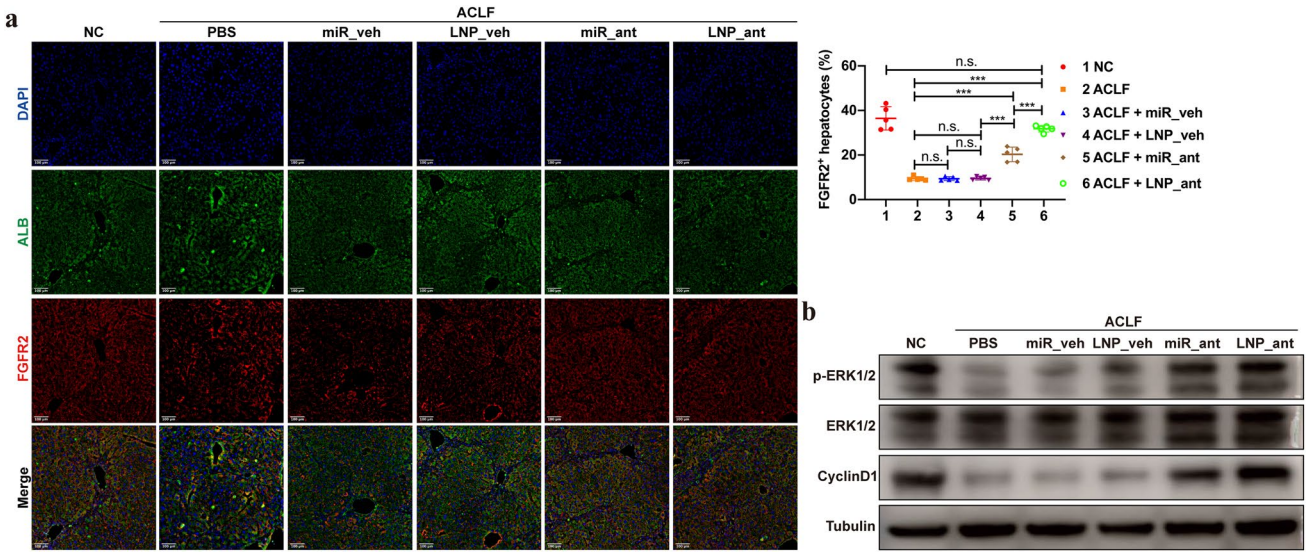

Fig. 7 Inhibition of miR-218-5p in the liver of ACLF mice could restore the expression of FGFR2. **a** Immunofluorescence staining showed that decreased expression of FGFR2 could partially restored when treated with miR-218-5p-antagomir and the effect enhanced when delivering by LNP ($n=5$). Scale bars, 100 μm. Quantitative presentation of FGFR2$^+$ hepatocytes were shown ($n=5$). **b** Western blotting showed that decreased expression of p-ERK1/2 and cyclinD1 in ACLF mice could reverse when treated with miR-218-5p-antagomir and the effect enhanced when delivering by LNP. One-way ANOVA was used for statistical evaluation (n.s., no significance; ***$p<0.001$). Data were presented as the mean ± SD. *ACLF* acute-on-chronic liver failure, *FGFR2* Fibroblast Growth Factor Receptor 2, *ALB* albumin, *DAPI* 4′,6-diamidino-2-phenylindole, *LNP* lipid nanoparticle, *miR_veh* miR-vehicle, *miR_ant* miR-antagomir, *LNP_veh* LNP-vehicle, *LNP_ant* LNP-antagomir

cells, cultured in vitro to regulate hepatocyte proliferation. However, EVs secreted by these cells did not reflect the true microenvironmental conditions of liver tissue, especially diseased liver tissue. Even EVs from primary hepatocytes could not adequately describe the true state of the liver microenvironment. Slight changes in the in vitro culture conditions might result in the corresponding changes in the EVs contents and their functions. Therefore, liver-derived EVs became an excellent tool for studying the pathophysiological changes in liver tissue. Surprisingly, liver-derived EVs from healthy and ALI mice could promote hepatocyte proliferation, which confirmed their ability to reflect the changes in the liver microenvironment promptly and accurately. Therefore, we extracted ACLF_EVs from the discarded diseased liver tissue of HBV-ACLF patients and injected them into ALI mice and found that ACLF_EVs inhibit liver regeneration, thereby delaying the repair of liver self-injury. This phenomenon was consistent with the impaired liver regeneration of ACLF, which usually occurred acutely based on liver cirrhosis. Long-term chronic liver injury was a major important cause of its impaired liver regeneration. Therefore, we extracted LC_EVs from discarded diseased liver tissue of HBV-LC patients, which revealed that similar to ACLF_EVs, LC_EVs also had the capacity to suppress liver regeneration. These outcomes demonstrated that liver-derived EVs had the power to reflect disease characteristics accurately and were significant disease markers, as well as potential directions for the development of new therapeutic approaches in the future.miRNAs are critical modulators of organisms involved in various pathophysiological processes. The abundance of miRNAs within EVs mediated their functions. The current study found that upregulated miR-218-5p within ACLF_EVs was a major factor in inhibiting liver regeneration. Previous studies suggested an essential association of miR-218-5p with tumor development [28]. Yu et al. found that miR-218-5p regulates the progression of hepatocellular carcinoma by reducing cancer proliferation, migration, and invasion and increasing the apoptosis of cancer cells [29]. However, the association of miR-218-5p with impaired liver regeneration in HBV-ACLF patients had not been reported. Herein, we revealed that miR-218-5p was highly expressed in ACLF_EVs and functioned as an inhibitor of hepatocyte proliferation and liver regeneration by suppressing the expression of FGFR2, inactivating the ERK1/2 pathway, and reducing the level of cyclinD1 in hepatocytes. Also, we analyzed the reason for elevation of miR-218-5p. First, we analyzed the miRNA sequencing data of HC_EVs, LC_EVs and ACLF_EVs (Supplementary Table S2). We found that the expression level of miR-218-5p within LC_EVs and ACLF_EVs were significantly improved and statistically significant compared to HC_EVs (LC_EVs/HC_EVs $\log_2$FC = 1.96 $p<0.01$ ACLF_EVs/HC_EVs $\log_2$FC = 2.54 $p<0.001$). However, the expression level of miR-218-5p within ACLF_EVs was somewhat elevated

compared to LC_EVs, but not statistically different (ACLF_EVs/LC_EVs $\log_2$FC = 0.70 p = 0.23). Next, we compared the expression levels of miR-218-5p in liver-derived EVs of HC mice, ALI mice, and 8-week chronic inflammatory stage ACLF mice. The results showed that the expression of miR-218-5p was mildly increased in ALI mice compared with HC mice (Fig. S5a), but there was no statistical difference, while it was significantly increased in ACLF mice at the chronic inflammation (CI) stage (Fig. S5a). In summary, we suggested that the increased miR-218-5p expression level in liver-derived EVs was mainly triggered by chronic inflammation. Thus, we promoted liver regeneration in ACLF mice by administering miR-218-5p-antagomir during chronic inflammation to reverse the high expression of miR-218-5p.

Blood-transported miRNAs were prone to degradation and could not be effectively enriched in specific organs, thus limiting their application. Therefore, selecting an appropriate delivery vehicle could enhance the therapeutic effect. LNP directed cell entry by interacting with lipoprotein E and were subsequently internalized into hepatocytes by endocytosis. Previous studies have shown that even fibrotic livers have a strong ability to internalize LNP [25]. Moreover, the ability of LNP to target hepatocytes in the liver could effectively deliver competitive inhibitors of miRNA into target hepatocytes, amplifying the therapeutic effect [26]. In this study, LNP as a delivery vehicle for miR-218-5p-antagomir was more effective in promoting liver regeneration in ACLF mice. Therefore, utilizing LNP as a vehicle to deliver nucleic acid molecules was a therapeutic pattern with a strong clinical translational potential.

Nevertheless, the present study had some limitations. The liver is a complex organ composed of several cell types. Almost all cells had the ability to secrete EVs. ACLF_EVs constitute a complex secreted by multiple cells, and the exact cells from which ACLF_EVs originate could not be identified. If the main cellular sources of ACLF_EVs and miRNA could be identified, we might have the opportunity to intervene against such target cells to regulate impaired liver regeneration. To rationalize this issue, we firstly analyzed the expression level of miR-218-5p in human liver tissues from ACLF and HC. The result revealed that the expression level of miR-218-5p was increased in ACLF liver tissues (Fig. S6a). Also, similar result was found in mouse liver tissues (Fig. S6a). It is well known that liver tissue is mainly composed of parenchymal and non-parenchymal cells, with hepatocytes occupying the vast majority of liver tissue. During the course of ACLF, hepatocytes are often struck by chronic inflammation and thus undergo pathological changes. Therefore, we hypothesized that the high expression of miR-218-5p in liver-derived EVs might be derived from damaged hepatocytes. Then, we dissociated mouse liver tissues into primary hepatocytes and other non-substantial cells and detected the intracellular expression level of miR-218-5p. The results suggested that the expression of miR-218-5p was significantly higher in primary hepatocytes of ACLF mice compared with HC (Fig. S6b), while no significant difference was seen in the expression of miR-218-5p in non-substantial cells (Fig. S6b). Therefore, we speculated that ACLF_EVs and miRNAs might mainly originate from hepatocytes. In addition, liver regeneration was correlated with various pathophysiological processes in vivo. In the present study, we suggested that ACLF_EVs inhibited liver regeneration by suppressing hepatocyte proliferation. However, whether ACLF_EVs affected liver regeneration by modulating immunity or through other pathways needs to be explored further. Finally, EVs have a complex composition. To validate the mechanism of impaired liver regeneration by ACLF_EVs, additional in-depth studies on vesicle components analysis, including multi-omics studies to identify vesicle proteins, mRNA, and lncRNA are imperative.

In conclusion, the current study revealed that ACLF_EVs had the ability to inhibit liver regeneration, and the upregulated miR-218-5p within them was an essential factor. Decreasing the expression of miR-218-5p by targeted delivery of miR-218-5p-antagomir could improve liver regeneration in ACLF mice. This suggested that ACLF_EVs and their intrinsic miRNAs might be significant causes of impaired liver regeneration in HBV-ACLF. Studies on ACLF_EVs and their complex components could help to further investigate the causes of impaired liver regeneration in HBV-ACLF and the development of novel therapeutic approaches.

Supplementary Information The online version contains supplementary material available at https://doi.org/10.1007/s12072-023-10513-0.

Acknowledgements The authors acknowledge the patients, study investigators, and coordinators for their contributions in this study.

Author contributions All authors contributed to the study conception and design. SZ, JY and KR designed research; SZ, JY and KR and JC performed research; LM, YY, ZL and ZZ carried data analysis; YQ, MC and HH supervised research; SZ, JY and KR wrote the paper. All authors approved the manuscript.

Funding This study was supported by the National Natural Science Foundation of China (82170646 to Hualian Hang), "Key Project" of Shanghai Jiao Tong University Medical-Industry Intersection (YG2021ZD10 to Hualian Hang), Clinical Research Innovation Cultivation Fund of Renji Hospital, School of Medicine, Shanghai Jiao Tong University (RJPY-DZX-006 to Hualian Hang).

Data availability Sequencing data generated in this study has been deposited at the National Omics Data Encyclopedia (NODE) under the accession code OEP004077 (https://www.biosino.org/node/project/detail/OEP004077).

Declarations

Conflict of interest Senquan Zhang, Jie Yu, Keqiang Rao, Jie Cao, Lijie Ma, Yeping Yu, Zhe Li, Zhaokai Zeng, Yongbing Qian,Mo Chen,

Hualian Hang have no relevant financial or non-financial interests to disclose.

Ethics approval and consent to participate All procedures followed were in accordance with the ethical standards of the responsible committee on human experimentation (Ethics Committee of Renji Hospital of Shanghai Jiao Tong University School of Medicine, China) and with the Helsinki Declaration of 1975, as revised in 2008. Informed consent was obtained from all patients for being included in the study.

References

1. Wu T, Li J, Shao L, Xin J, Jiang L, Zhou Q, et al. Development of diagnostic criteria and a prognostic score for hepatitis B virus-related acute-on-chronic liver failure. Gut 2018;67:2181–2191
2. Arroyo V, Moreau R, Jalan R. Acute-on-chronic liver failure. N Engl J Med 2020;382:2137–2145
3. Sarin SK, Choudhury A. Acute-on-chronic liver failure: terminology, mechanisms and management. Nat Rev Gastroenterol Hepatol 2016;13:131–149
4. Belli LS, Duvoux C, Artzner T, Bernal W, Conti S, Cortesi PA, et al. Liver transplantation for patients with acute-on-chronic liver failure (ACLF) in Europe: results of the ELITA/EF-CLIF collaborative study (ECLIS). J Hepatol 2021;75:610–622
5. Michalopoulos GK. Hepatostat: Liver regeneration and normal liver tissue maintenance. Hepatology (Baltim, MD) 2017;65:1384–1392
6. Fausto N. Liver regeneration and repair: hepatocytes, progenitor cells, and stem cells. Hepatology (Baltim, MD) 2004;39:1477–1487
7. Xiang X, Feng D, Hwang S, Ren T, Wang X, Trojnar E, et al. Interleukin-22 ameliorates acute-on-chronic liver failure by reprogramming impaired regeneration pathways in mice. J Hepatol 2020;72:736–745
8. van Niel G, D'Angelo G, Raposo G. Shedding light on the cell biology of extracellular vesicles. Nat Rev Mol Cell Biol 2018;19:213–228
9. Luo C, Xin H, Zhou Z, Hu Z, Sun R, Yao N, et al. Tumor-derived exosomes induce immunosuppressive macrophages to foster intrahepatic cholangiocarcinoma progression. Hepatology (Baltim, MD) 2022;76:982–999
10. Nojima H, Freeman CM, Schuster RM, Japtok L, Kleuser B, Edwards MJ, et al. Hepatocyte exosomes mediate liver repair and regeneration via sphingosine-1-phosphate. J Hepatol 2016;64:60–68
11. Tan CY, Lai RC, Wong W, Dan YY, Lim S-K, Ho HK. Mesenchymal stem cell-derived exosomes promote hepatic regeneration in drug-induced liver injury models. Stem Cell Res Ther 2014;5:76
12. Kakizaki M, Yamamoto Y, Nakayama S, Kameda K, Nagashima E, Ito M, et al. Human hepatocyte-derived extracellular vesicles attenuate the carbon tetrachloride-induced acute liver injury in mice. Cell Death Dis 2021;12:1010
13. Wang J, Li L, Zhang Z, Zhang X, Zhu Y, Zhang C, et al. Extracellular vesicles mediate the communication of adipose tissue with brain and promote cognitive impairment associated with insulin resistance. Cell Metab 2022;34(1264–1279): e8
14. Lee J, Kim SR, Lee C, Jun YI, Bae S, Yoon YJ, et al. Extracellular vesicles from in vivo liver tissue accelerate recovery of liver necrosis induced by carbon tetrachloride. J Extracell Vesicles 2021;10: e12133
15. Sato K, Meng F, Glaser S, Alpini G. Exosomes in liver pathology. J Hepatol 2016;65:213–221
16. Wang X, He Y, Mackowiak B, Gao B. MicroRNAs as regulators, biomarkers and therapeutic targets in liver diseases. Gut 2021;70:784–795
17. Ng R, Song G, Roll GR, Frandsen NM, Willenbring H. A microRNA-21 surge facilitates rapid cyclin D1 translation and cell cycle progression in mouse liver regeneration. J Clin Investig 2012;122:1097–1108
18. Chang YM, Chen PC, Hsu CP, Ma PF, Chen HL, Hsu SH. Loss of hepatic miR-194 promotes liver regeneration and protects from acetaminophen-induced acute liver injury. Biochem Pharmacol 2022;195: 114862
19. Wen Y, Peng SF, Fu L, Fu XY, Wu DX, Liu BJ, et al. Serum levels of miRNA in patients with hepatitis B virus-associated acute-on-chronic liver failure. Hepatobiliary Pancreat Dis Int 2018;17:126–132
20. Tao YC, Wang ML, Wang M, Ma YJ, Bai L, Feng P, et al. Quantification of circulating miR-125b-5p predicts survival in chronic hepatitis B patients with acute-on-chronic liver failure. Dig Liver Dis 2019;51:412–418
21. Crescitelli R, Lasser C, Lotvall J. Isolation and characterization of extracellular vesicle subpopulations from tissues. Nat Protoc 2021;16:1548–1580
22. Xu D, Chen L, Chen X, Wen Y, Yu C, Yao J, et al. The triterpenoid CDDO-imidazolide ameliorates mouse liver ischemia-reperfusion injury through activating the Nrf2/HO-1 pathway enhanced autophagy. Cell Death Dis 2017;8:e2983
23. Ray AT, Mazot P, Brewer JR, Catela C, Dinsmore CJ, Soriano P. FGF signaling regulates development by processes beyond canonical pathways. Genes Dev 2020;34:1735–1752
24. Tian ZJ, An W. ERK1/2 contributes negative regulation to STAT3 activity in HSS-transfected HepG2 cells. Cell Res 2004;14:141–147
25. Yang T, Poenisch M, Khanal R, Hu Q, Dai Z, Li R, et al. Therapeutic HNF4A mRNA attenuates liver fibrosis in a preclinical model. J Hepatol 2021;75:1420–1433
26. Gokita K, Inoue J, Ishihara H, Kojima K, Inazawa J. Therapeutic potential of LNP-mediated delivery of miR-634 for cancer therapy. Mol Ther Nucleic Acids 2020;19:330–338
27. Engelmann C, Habtesion A, Hassan M, Kerbert AJ, Hammerich L, Novelli S, et al. Combination of G-CSF and a TLR4 inhibitor reduce inflammation and promote regeneration in a mouse model of ACLF. J Hepatol 2022;77:1325–1338
28. Deng M, Zeng C, Lu X, He X, Zhang R, Qiu Q, et al. miR-218 suppresses gastric cancer cell cycle progression through the CDK6/Cyclin D1/E2F1 axis in a feedback loop. Cancer Lett 2017;403:175–185
29. Yu J, Yang M, Zhou B, Luo J, Zhang Z, Zhang W, et al. CircRNA-104718 acts as competing endogenous RNA and promotes hepatocellular carcinoma progression through microRNA-218-5p/TXNDC5 signaling pathway. Clin Sci (Lond) 2019;133:1487–1503